ELSEVIER

ADVANCES IN NEURAL NETWORK RESEARCH

IJCNN 2003

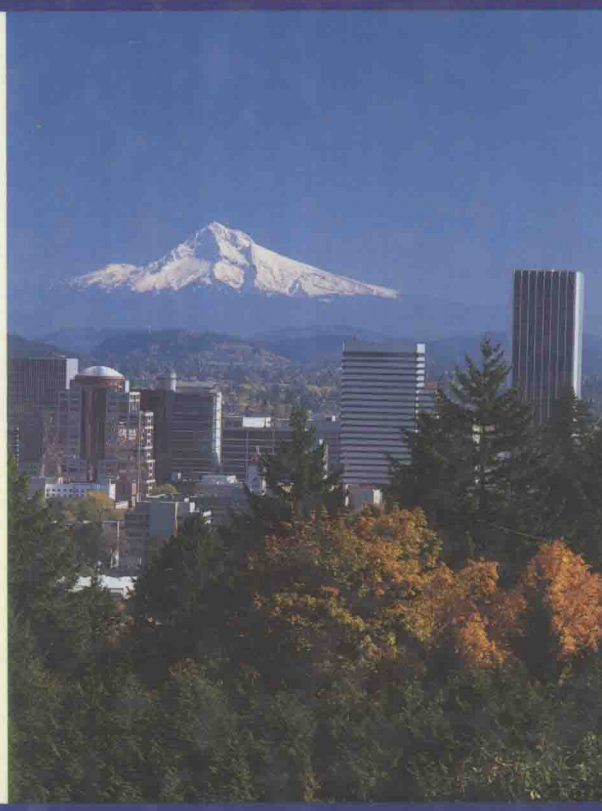

DONALD C. WUNSCH II
MICHAEL E. HASSELMO
GANESH KUMAR VENAYAGAMOORTHY
DELIANG WANG
Editors

IEEE

ADVANCES IN NEURAL NETWORKS RESEARCH IJCNN 2003

Edited by

Donald C. Wunsch II
University of Missouri-Rolla

Michael Hasselmo
Boston University

Ganesh Kumar Venayagamoorthy
University of Missouri-Rolla

DeLiang Wang
Ohio State University

Pergamon

Amsterdam - Boston - Heidelberg - London -Oxford - Paris
San Diego - San Francisco - Singapore - Sydney - Tokyo

ELSEVIER SCIENCE Ltd
Pergamon (an imprint of Elsevier Science)
The Boulevard, Langford Lane
Kidlington, Oxford OX5 1GB, UK

First edition 2003

Library of Congress Cataloging in Publication Data
A catalog record from the Library of Congress has been applied for.

British Library Cataloguing in Publication Data
A catalogue record from the British Library has been applied for.

Advances in Neural Network Research: IJCNN 2003. Edited by Donald C. Wunsch II, Mike Hasselmo, Ganesh Kumar Venayagamoorthy and DeLiang Wang. Reprinted from Neural Networks, Volume 16, Nos. 5-6 (2003)

Photo on the front cover by Steve Terrill. (www.terrillphoto.com)

ISBN: 0 08 044320 6

♾ The paper used in this publication meets the requirements of ANSI/NISO Z39.48-1992 (Permanence of Paper).
Printed in Great Britain.

NEURAL NETWORKS

CONTENTS

2003 Special Issue: Advances in Neural Networks Research – IJCNN'03

Preface: The Best of the Best

The top-reviewing papers from the 2003 International Joint Conference on Neural Networks (IJCNN) have been expanded and assembled here in book format. In odd-numbered years, IJCNN is led by the INNS, and in even-numbered years, by the IEEE. This year, we decided to offer this select group of IJCNN authors a chance to expand their papers. The chapters of this book appeared as a special issue of the *Neural Networks* journal in July 2003.

IJCNN is the flagship conference of the INNS, as well as the IEEE Neural Networks Society. It has arguably been the pre-eminent conference in the field, even as neural network conferences have proliferated and specialized. As the number of conferences has grown, its strongest competition has migrated away from an emphasis on neural networks. IJCNN has embraced the proliferation of spin-off and related fields (see the topic list, below), while maintaining a core emphasis befitting its name. It has also succeeded in enforcing an emphasis on quality. While being an inclusive conference, IJCNN has strict standards for acceptance, including literature review, quality of English; and reproducibility, accuracy and meaningfulness of results. All papers, even invited papers, were subject to a minimum of two reviews -- and many papers received up to five. We rejected 15% of submitted papers, and only the top 10% of the remaining papers are presented in this issue. These topics cover most of the major areas of research in neural networks, including: self-organizing maps, reinforcement learning, support vector machines, adaptive resonance theory, principal component analysis and independent component analysis, as well as numerous engineering applications and detailed biological models of the function of neural circuits.

IJCNN '03 has, at this writing, surpassed expectations in every capacity. We got all our first choices of plenary speakers: Kunihiko Fukushima, Earl Miller, Terrence Sejnowski, Vladimir Vapnik, and Christoph von der Malsburg; an extraordinary slate of tutorial presenters, and 730 submitted articles -- 33% over projections. Papers are presented in 20-minute format in four parallel sessions, planned to be as topically orthogonal as possible. Poster presentations are given their own generous time slot as well.

If you haven't been to IJCNN lately, you don't know what you are missing. For more information, see www.ijcnn.net or www.inns.org or www.ieee-nns.org. It has been our pleasure to work on creating the program for IJCNN, as well as this book, for you.

Sincerely,

Donald C. Wunsch II, University of Missouri-Rolla
General Chair, IJCNN '03
Michael E. Hasselmo, Boston University
Program Chair, IJCNN' 03
Ganesh Kumar Venayagamoorthy, University of Missouri-Rolla
Program Co-Chair, IJCNN '03
DeLiang Wang, Ohio State University
Program Co-Chair, IJCNN '03

2003 International Joint Conference on Neural Networks
TOPIC LIST

A. PERCEPTUAL AND MOTOR FUNCTION
Vision and image processing
Pattern recognition
  Face recognition
  Handwriting recognition
  Other pattern recognition
Auditory and speech processing
  Audition
Speech recognition
  Speech production
  Other perceptual systems
  Motor control and response
B. COGNITIVE FUNCTION
Cognitive information processing
Learning and memory
Spatial Navigation
Conditioning, Reward and Behavior
Mental disorders
Attention and Consciousness
Language
Emotion and Motivation
C. COMPUTATIONAL NEUROSCIENCE
Models of neurons and local circuits
Systems neurobiology and neural modeling
Spiking neurons
D. INFORMATICS
Neuroinformatics
Bioinformatics
Artificial immune systems
Data mining
E. HARDWARE
Neuromorphic hardware and implementations
Embedded neural networks
F. REINFORCEMENT LEARNING AND CONTROL
Reinforcement learning
Approximate/Adaptive dynamic programming
Control
Reconfigurable systems
Robotics
Fuzzy neural systems
Optimization
G. DYNAMICS
Neurodynamics
Recurrent networks
Chaos and learning theory
H. THEORY
Mathematics of Neural Systems
Support vector machines
Extended Kalman filters
Mixture models, EM algorithms and ensemble learning
Radial basis functions
Self-organizing maps
Adaptive resonance theory
Principal component analysis and independent component analysis
Probabilistic and informationtheoretic methods
Neural Networks and Evolutionary Computation
I. APPLICATIONS
Signal Processing
Telecommunications
Applications
Time Series Analysis
Biomedical Applications
Financial Engineering
Biomimetic applications
Computer security applications
Power system applications
Aeroinformatics
Diagnostics and Quality Control
Other applications

PERGAMON

AVAILABLE AT
www.ComputerScienceWeb.com
POWERED BY SCIENCE DIRECT

Neural Networks 16 (2003) 521–528

Neural Networks

www.elsevier.com/locate/neunet

2003 Special issue

Adaptive force generation for precision-grip lifting by a spectral timing model of the cerebellum

Antonio Ulloa*, Daniel Bullock, Bradley J. Rhodes

Department of Cognitive & Neural Systems, Boston University, 677 Beacon Street, Boston, MA 02215, USA

Abstract

We modeled adaptive generation of precision grip forces during object lifting. The model presented adjusts reactive and anticipatory grip forces to a level just above that needed to stabilize lifted objects in the hand. The model obeys principles of cerebellar structure and function by using slip sensations as error signals to adapt phasic motor commands to tonic force generators associated with output synergies controlling grip aperture. The learned phasic commands are weight- and texture-dependent. Simulations of the new circuit model reproduce key aspects of experimental observations of force application. Over learning trials, the onset of grip force buildup comes to lead the load force buildup, and the rate-of-rise of grip force, but not load force, scales inversely with the friction of the object.

Keywords: Adaptive timing; Neural model; Synaptic plasticity; Prehension; Learning; Force

1. Introduction

Grasping, lifting, and replacing an object require timed application of *grip forces* (to stabilize the object in the hand during object transport) and *load forces* (to elevate/lower the arm–object system to desired heights in the gravity field). An episode of lifting and lowering an object from and to a table top involves (Johansson, 1996; Johansson & Westling, 1987; Wing, 1996): *pre-lifting*, using the fingers to apply force perpendicular to the object's surface at the points of contact of the fingers with the object; *lifting*, which involves continuing increase of grip force and simultaneous application of load forces sufficient to vertically displace the arm/object system, and to halt its motion at the desired height; *holding* by maintaining grip and load forces; *controlled lowering*, by reducing load forces below the value needed to counteract gravity; and *release*, by rapid simultaneous decrease of grip and load forces following object contact with the table.

After reviewing data on precision grip and prior models of grip force control, this paper presents simulations of a new mathematical model of the neural circuit that enables actors to learn to generate appropriate grip forces to prevent object slippage during lifting. Such learning involves a transition from *reactive* to primarily *anticipatory* application of grip forces that reflect the weight and texture of the object. Also addressed are the problems of reactive load force generation and temporal coordination between load and grip force generation.

2. Data on precision grip

This section outlines: roles of motor cortex and cerebellum in precision grip; trends in the relative timing of exertion of load force versus grip force; and trends in the dependence of grip force on object weight and texture.

2.1. Motor cortex and cerebellum in precision grip

Cell recordings and functional imaging of activity in primary motor cortex (MI) have established close links between MI activity and precision grip force (e.g. Lemon, Johansson, & Westling, 1995; Maier, Bennett, Hepp-Reymond, & Lemon, 1993). Complete lesion of MI and somatosensory cortex impaired monkeys' ability to pick up food that could only be accessed with precision grip (Passingham, 1993). Whereas pre-lesion monkeys used precision grip, post-lesion monkeys retrieved food using whole-hand prehension. Reversible inactivation of MI by

* Corresponding author. Address: National Institutes of Health, Brain Imaging & Modeling Section, 9000 Rockville Pike, 10/3C716, Bethesda, MD 20892, USA. Tel.: +1-301-435-5141; fax: +1-301-480-5625.

E-mail addresses: antonio.ulloa@nih.gov; aup@cns.bu.edu (A. Ulloa), danb@cns.bu.edu (D. Bullock), brhodes@cns.bu.edu (B.J. Rhodes).

0893-6080/03/$ - see front matter
doi:10.1016/S0893-6080(03)00004-7

injection of a GABA agonist produced a similar deficit (Brochier, Boudreau, Pare, & Smith, 1999). Such results exemplify the principle (Passingham, 1993) that MI enables *selective* activation of one or a few effectors, e.g. single joints or fingers, when many effectors could contribute.

Inactivation of the dentate nucleus of the cerebellum, which projects to MI via the thalamus, severely impairs precision grip. After GABA agonist injection in dentate, monkeys used only one finger to retrieve food from a hole, instead of the thumb-index strategy used before (Thach, Goodkin, & Keating, 1992). This effect probably depends partly on disrupted dentate input to MI. Inactivation of the dentate leads to a loss of anticipatory phasic components of MI cell discharges (Vilis & Hore, 1980). Loss of anticipatory components of precision grip, which requires two-finger coordination, may have so degraded the grip that the animal chose the simpler, one-finger, strategy. Consistently (Serrien & Wiesendanger, 1999), patients with unilateral cerebellar damage showed timed, ramp-like anticipatory grip force adjustments on the unaffected side, but maintained high grip forces on the affected side. Switching from an efficient, phasic strategy to a costly tonic strategy may result from loss of the cerebellar adaptive timing needed for the more efficient strategy.

The intermediate zone of cerebellar cortex, which dominates the nucleus interpositus (NIP), also shows strong activity modulation during precision grip. A majority of Purkinje cells in this zone responded with a decrease in tonic activity during maintained grasping (Smith & Bourbonnais, 1981). This decrease would disinhibit the NIP cells, whose resultant excitatory responses could act via the red nucleus, or via motor thalamus and MI, to generate a force increase.

Sufficient repetition of predictable slip events generates anticipatory discharges in NIP-controlling cerebellar cortex neurons. Dugas and Smith (1992) trained monkeys to grasp an object and hold it in a fixed vertical position for 1 s. During a block of trials called slip perturbation trials, a downward force was briefly applied to the object after it had been kept at the correct vertical position for 750 ms. The monkey prevented the object from moving outside a narrow range of vertical heights by phasically stiffening its wrist and firming its grip. On perturbation trials, there was a reflex response evidenced by increases in hand muscle activity and by modulation of discharge in Purkinje and unidentified cells in the paravermal anterior lobe of the cerebellum. Activity increased in muscles with a 30–50 ms latency, and peaked at 50–100 ms *after* the perturbation. About half of the recorded Purkinje cells increased or decreased their simple spike discharges at about 45 ms after the perturbation. Most of the Purkinje cells that responded to the perturbation had cutaneous receptive fields.

After a series of perturbations, a grip force increase, and an *increase* in Purkinje cell activity, developed in *anticipation* of the perturbation, which occurred reliably 750 ms after the cue tone. Grip force began to diverge upward relative to control levels 450 ms before the expected perturbation, and a number of the Purkinje cells increased their discharge at least 50 ms before the grip force divergence. As anticipatory discharges developed, the same cells decreased their reactive, post-perturbation discharge (rendered unnecessary by the effectiveness of the anticipatory response). None of the Purkinje cells exhibited perturbation-related complex spikes, which if present would indicate excitation of Purkinje cells by climbing fiber (CF) discharges. The absence of slip-related CF discharges (in the Purkinje cells studied) may explain why anticipatory *increases* were observed in these Purkinje cell responses rather than anticipatory *reductions*. Many other studies of cerebellar activity have indicated that learned increments in some Purkinje cells' activities typically coincide with learned decrements in others (Berthier & Moore, 1986). Long-term depression (LTD) of excitatory parallel fiber (PF) inputs to Purkinje cells depends on coincidence between two inputs to Purkinje cells: predictive state/context signals carried by PFs and (putative error) signals carried by perturbation-locked CF discharges (Hansel, Linden, & D'Angelo, 2001). Long-term potentiation (LTP) occurs when predictive stimuli excite Purkinje cells in the absence of coincident CF discharges (Hansel et al., 2001). Both LTD and LTP can promote grip force increments if they occur in separate command pathways for opponent muscles. CF discharges in response to cutaneous slip have been reported (Gellman, Gibson, & Houk, 1985).

2.2. Timing and variation of precision grip force

Timing of grip force with respect to load force. In Johansson and Westling (1984), subjects grasped and lifted a 400 g object to about 2 cm above a table top, held it suspended for 10 s, and then replaced it. On some trials, the subjects (Ss) were asked to slowly let the object fall, in order to measure that force level, called the *slip force*, at which the object would slip from the fingers. On typical lift–hold–replace trials, the following *phases* were observed: (1) One of the fingers first touched the object ~50 ms before the first application of grip force. (2) Grip force increased but not load force. This period lasted 80 ± 40 ms. (3) Grip and load forces increased in parallel. (4) Gravity force was overcome, and the object lifted, until it reached the intended height. In this period, grip force reached its maximum value during a transient overshoot of its steady state. (5) Grip and load forces stabilized while Ss held the object in the air. (6) A reduction of load force allowed the object's position to slowly approach the tabletop. (7) At contact, grip and load forces were synchronously terminated.

Rate of rise of grip force during pre-lifting is a function of object weight. The rate of rise of grip force during prelifting is greater for heavier objects (Johansson & Westling, 1988).

Rate of rise of grip force during pre-lifting is a function of object texture. More slippery objects induced faster rates of pre-lift grip force development. In marked contrast, the rate of rise of load force was the same for all textures (Johansson & Westling, 1984).

Grip force during lifting is a joint function of the surface texture and weight of the object lifted (Westling & Johansson, 1984). The static grip force (grip force maintained during the holding stage) was an increasing function of object weight, as was (of course) the minimal force required to prevent slipping (slip force). A greater grip force was used when the material was more slippery.

The time to attain a level of grip force adequate for a given weight/texture is nearly constant for all weights and textures (Johansson & Westling, 1984, 1988). Such constancy greatly reduces variability of behavioral timing.

3. Prior models of grip force control

Johansson (1996) proposed a conceptual model for the application of grip forces and load forces in a lifting task. Briefly, vision provides information on object position, object size, and object shape. This information is used to activate controllers for transporting the hand towards the object while the fingers are being preshaped. Based on visual estimates of weight and friction, a set of tactile responses is predicted to guide planning for the application of initial grip force to the object. Tactile perceptions of weight and texture are fed back and compared to the predicted weight and texture. The mismatch is used to update memory representations of weight and texture for a specific object appearance. This memory is assumed to be retrieved on later occasions to guide anticipatory application of forces (Gordon, Westling, Cole, & Johansson, 1993). If a declining grip force results in slip, a resulting slip alert signal in hand mechanoreceptors triggers a reactive increase in grip force.

Fagergren, Ekeberg, and Forssberg (2000) modeled the transfer function of the peripheral motor system involved in application of grip force. To measure properties of an *active* increase in grip force, subjects were instructed to voluntarily increase grip force in a step-like fashion (from 1 to 50% of maximum voluntary contraction). To test the *reactive* component of grip force, the weight of the object was unexpectedly increased. Once a transfer function for each experiment was identified, a third transfer function was composed to describe a common system involved in active and reactive force generation.

4. A new model of grip force control

Prior treatments of grip force control (Fagergren et al., 2000; Gordon et al., 1993; Johansson, 1996) have not modeled the neural substrates of adaptive control. This section introduces a new, neurobiologically interpretable, model that formalizes the role of MI and the cerebellum in learned transitions from reactive to anticipatory application of grip forces whose magnitudes are texture- and weight-dependent. Control is exercised in aperture coordinates because once the fingers enclose and touch the object, the *targeted* hand aperture can be voluntarily decreased by a further amount. Decreasing the targeted aperture to a value less than object width would cause the fingers to try to move beneath the object's surface, thereby building up a force on it. The size of the applied force would be a function of the size of the decrement (below object width) of target aperture, and of joint stiffness, control of which has been modeled elsewhere (Bullock & Contreras-Vidal, 1993).

4.1. Model circuit and its operation during learning

A model circuit that learns to generate and apply context-dependent grip forces in anticipation of load force application is shown in Fig. 1. It works as follows. Before learning, there is a significant slip error, ε_A, the magnitude of which is needed as an input for the model. As shown at

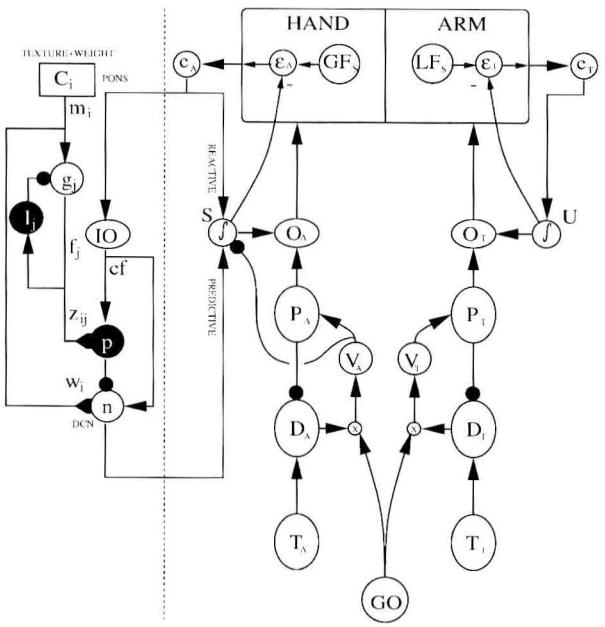

Fig. 1. Circuit for learned transition between reactive and anticipatory grip forces. Elements to the left of the dashed line are components of a cerebellar side-loop that includes inputs from the pons and the inferior olive. Elements to the right of the dashed line are cortical parts of the grip and load force generators and the error estimators. Key: C_i, pontine context representation signals for texture and weight; m_i, mossy fiber signal; g_i, granule cell; l_j, Golgi cell; f_j, parallel fiber signal; IO, inferior olive; cf, climbing fiber; z_{ij} and w_i, weights at adaptive synapses; n, deep cerebellar nuclear (DCN) cell; O_A and O_T, outflow force position vectors for aperture and transport components; S, integrator for grip force adjustments and U, integrator for load force generation; e_A, delayed slip error; e_T, delayed load error; ε_A, slip error; ε_T, load error; GFs, minimal grip force to avoid slip; LFs, appropriate load force to overcome object weight.

the top of Fig. 1, ε_A was computed as the difference between GF_S, the minimal grip force necessary to prevent slip, and the current net adjustment, S, to grip force. Input ε_A is tracked by cell activation variable e_A to form an internal estimate of slip error in the frame of the hand. The figure shows that current net adjustment S is the integral of two phasic inputs: a reactive input from cell e_A and a learned anticipatory input from cell n. The net adjustment S acts on the hand via aperture/force command O_A.

A cerebellar circuit (left side of Fig. 1) enables the model to learn how to preempt performance errors. In addition to providing phasic feedback to charge O_A, cell e_A sends an error signal to the inferior olive, IO, to phasically activate CF signals, *cf*. Because CF branches reach both the cerebellar cortex and the deep cerebellar nuclear (DCN) cells, the *cf* signals excite the Purkinje cell dendritic tree (p) and the DCN cells (n) inhibited by the Purkinje cell.

A context signal, C_i, from the pons, corresponds to the decision to lift the object with the weight-texture combination indexed by i. Signal C_i activates mossy fibers (MF) m_i, each of which in turn generates a spectrum of granule cell activations, g_j. This spectrum of activations, inhibited by Golgi interneuron activities l_j, generates phasic PF activities f_j with different rise times and amplitudes (Bullock, Fiala, & Grossberg, 1994). Adaptive synapses z_{ij} from PFs to Purkinje cells undergo LTD when PF activations are repeatedly paired with CF activations $h(e_A)$. In addition, these synapses undergo long-term potentiation (LTP, slower than LTD) when PF signals f_j are present but there are no correlated CF signals. There are also adaptive synapses, w_i, from MFs to nuclear cells; these synapses undergo LTP when MF activation is paired with CF activation $h(e_A)$; LTD (slower than LTP in these synapses w_i) occurs when MFs are activated without coincident CF activation. Purkinje cells have a baseline activation that normally inhibits the DCN cell. The DCN cell is gradually, and context-dependently, released from this inhibition as the PF-Purkinje cell synapses z_{ij} undergo LTD, because this reduces excitatory inputs to Purkinje cells while inhibitory inputs are maintained. Whenever the C_i cue is presented, the resultant phasic reduction of Purkinje cell inhibition of DCN cells allows the DCN cell activation to express a learned compensation for (what would otherwise be) a forthcoming error. The signal n from the DCN cell reaches the command stage O_A following summation with e_A and integration to form net compensation S. When a command is sent to *increase* the hand aperture T_A, and thus *release* the grip on the object, the integrators must be reset in order to zero the grip force adjustments. Fig. 1 shows that reset in the model is mediated by inhibition of the integrator S whenever there is a positive (opening) aperture velocity command, V_A.

In order to generate a load force that depends on weight-related movement errors in the transport component, a corresponding outflow force position vector in the transport component (O_T in the figure) was introduced, which also receives force adjustments from an integrator, U. As in the Vector Integration To Endpoint model (Bullock, Cisek, & Grossberg, 1998) of MI contributions in arm movement control, O_T cells provide graded force application modulated by integrated feedback of movement error based on signals arising in muscle spindles. Fig. 1 shows that U integrates e_T and e_T tracks the movement error, ε_T. The input ε_T is computed as the difference between the minimal load force, LF_S, adequate for the given object weight, and the current load force, U.

4.2. Technical specifications of the model

Arm transport component. The arm transport component of Fig. 1 obeys the following equations (Cf. Bullock et al., 1998; Ulloa & Bullock, 2003):

$$\dot{D}_T = \alpha(-D_T + T_T - P_T) \tag{1}$$

$$\dot{V}_T = \alpha_V(-V_T + G[D_T]^+) \tag{2}$$

$$\dot{P}_T = V_T \tag{3}$$

and

$$O_T = P_T + U \tag{4}$$

where D_T is the transport difference vector (positive values only when rectified via $[D_T]^+$), $\dot{D}_T$ is the time derivative of D_T, T_T is the internal representation of the position of the target, P_T is the transport present position vector, V_T is a velocity command vector, and GO signal G initiates movement. Parameters α and α_V were set to 30 and 300, respectively. O_T is the outflow force position vector for the transport component, and U integrates the load error:

$$\dot{U} = \alpha_U e_T \tag{5}$$

where α_U was set to 40. In this study, 1D vectors were sufficient to represent stages in the control of the elbow flexion needed to lift the object.

Grip aperture component. The grip aperture component obeyed the following system of equations:

$$\dot{D}_A = \alpha(-D_A + T_A - P_A) \tag{6}$$

$$\dot{V}_A = \alpha_V(-V_A + GD_A) \tag{7}$$

$$\dot{P}_A = V_A \tag{8}$$

and

$$O_A = P_A - S \tag{9}$$

where D_A is the difference vector for hand aperture, T_A is the internal vector representation of the target aperture, P_A is the aperture present position vector, V_A is the aperture velocity vector; O_A is the outflow force-position vector; S is defined by

$$\dot{S} = \alpha_S(e_A + [n]^+ - \beta_S[V_A]^+ S) \tag{10}$$

where e_A is the slip error signal (which tracks ε_A) and n is the nuclear (DCN) cell activity. Here again, 1D vectors sufficed for current purposes. The term $-\beta_S[V_A]^+S$ resets the integration of the reactive and predictive adjustments to grip force, by causing a decay in cell S whenever the aperture velocity cell, V_A, is positive. This reset is needed to implement releases of grip force, by eliminating the slip-preventing grip adjustments and allowing the aperture to relax. The rate term α_S was set equal to 40 and β_S to 3.

GO signal. The GO signal generator is defined as:

$$\dot{G} = \alpha_G(-G + G_0(t)) \tag{11}$$

where

$$G_0(t) = g_0 t^{1.4} \tag{12}$$

and $\alpha_G = 30$. G is the GO signal multiplying the difference vector of each component (Eqs. (2) and (7)), and g_0 is a step input from a decision center in the brain.

Slip error. The slip error, ε_A, starts being integrated by e_A at 0.050 s after the onset of the GO signal, to account for the delay between onset of muscle activation and onset of slip signals from mechanoreceptors. The delayed slip error is defined by

$$\dot{e}_A = \alpha_{e_A}(-e_A + \gamma_{e_A}[\varepsilon_A]^+) \tag{13}$$

where $\alpha_{e_A} = 50$. Factor $\gamma_{e_A} = 0.08$ scales the slip error, ε_A, which is approximated by

$$\varepsilon_A \propto \mathrm{GF}_S(u, v) - S. \tag{14}$$

Here GF_S is the minimal grip force needed to prevent slip of an object of weight u and texture v.

Load error. The load force error for the transport component, ε_T, starts being integrated by e_T at 0.050 s after the onset of the GO signal, to account for the delay in detecting load error. The delayed load error is defined by

$$\dot{e}_T = \alpha_{e_T}(-e_T + \gamma_{e_T}[\varepsilon_T]^+) \tag{15}$$

where $\alpha_{e_T} = 50$; $\gamma_{e_T} = 0.25$ scales the error, ε_T, which is approximated by

$$\varepsilon_T \propto \mathrm{LF}_S(u) - U \tag{16}$$

where LF_S is a load force adequate for an object of weight u.

Cerebellar component. This component follows the cerebellar timing model developed by Bullock et al. (1994) for eye blink conditioning (cf. also Rhodes & Bullock, 2002). This is one of the simplest models that give the needed computations, viz.: learning with any interstimulus interval (ISI) in the range [0.1 s, 4 s] and timed generation of a context-specific response of sufficient size to preempt the expected error.

A phasic context signal, C_i, activated at $t = -0.200$ s, excites cell activities, m_i, carried by MFs:

$$\dot{m}_i = -\alpha_m m_i + \beta_m(1 - m_i)(C_i + m_i) \tag{17}$$

where $\alpha_m = 0.2$ and $\beta_m = 10$; the positive feedback in Eq. (17) allows the network to keep a trace of C_i in short-term memory. MFs are directed to two classes of cells, granule cells and DCN cells. Granule cells were defined as

$$\dot{g}_j = \alpha_j((1 - g_j)m_i - \beta_g(g_j + \gamma_g)l_j) \tag{18}$$

where α_j is the rate of activation, drawn from the interval [1.3, 12], of the jth granule cell, where $j = 1, 2, \ldots, 40$, $\beta_g = 4$, and $\gamma_g = 0.1$. Signal l_j is a feedback inhibition of granule cells by Golgi cells:

$$\dot{l}_j = -\alpha_l l_j + \beta_l(1 - l_j)(\gamma_l m_i + f_j) \tag{19}$$

where $\alpha_l = 0.1$, $\beta_l = 5$, and $\gamma_l = 0.02$. The use of f_j in Eq. (19) and l_j in Eq. (18) together imply recurrent signal processing in the cerebellar cortex. The signals f_j conducted by PFs were

$$f_j = \frac{b([g_j - \lambda_f]^+)^2}{1 + c([g_j - \lambda_f]^+)^2} \tag{20}$$

where $b = 12$, $c = 4$, and $\lambda_f = 5$.

Signals f_j are directed to a Purkinje cell through synapses, z_{ij}, which adapt according to

$$\dot{z}_{ij} = f_j((1 - z_{ij}) - \beta_z h(e_A)z_{ij}) \tag{21}$$

where the learning rate $\beta_z = 10$. Thus weights z_{ij} can exhibit slow LTP via term $f_j(1 - z_{ij})$ and faster LTD via term $f_j\beta_z h(e_A)z_{ij}$. The LTD process is gated by CF signal

$$h(e_A) = \begin{cases} e_A & \text{if } \dot{e}_A \geq 0 \\ 0 & \text{otherwise.} \end{cases} \tag{22}$$

This function provides a means to use only the leading edge of the slip error signal e_A. This is justified by evidence (Ito, 1984) that the IO provides this type of filtering. The Purkinje cell firing rate was defined as

$$p = 1 + \frac{1.5\ \mathrm{sgn}(b)b^2}{1 + b^2} \tag{23}$$

where $b = J^+ - J^-$ is the net activity on the dendrites of the Purkinje cells. Here the excitatory term

$$J^+ = \sum_{k=1}^{N} f_k z_{ik} \tag{24}$$

and the inhibitory term

$$J^- = \sum_{k=1}^{N} f_k s_{ik} \tag{25}$$

where $N = 40$. Term J^- represents the influence of basket and stellate cells on the Purkinje cell. For present purposes, the sum in (Eq. 25) had a constant value of 1.0. MFs are also

directed to the DCN cell, whose activity, n, was defined by

$$\dot{n} = \alpha_n\left(-n + \sum_{i=1}^{M} m_i w_i - p\right) \tag{26}$$

where M is the number of different context cues and $\alpha_n = 100$. The adaptive synapses, w_i, from MFs to nuclear cells were adapted according to

$$\dot{w}_i = m_i(\alpha_w w_i + \beta_w(1 - w_i)h(e_A)) \tag{27}$$

where the forgetting rate $\alpha_w = -0.001$ and the learning rate $\beta_w = 10$.

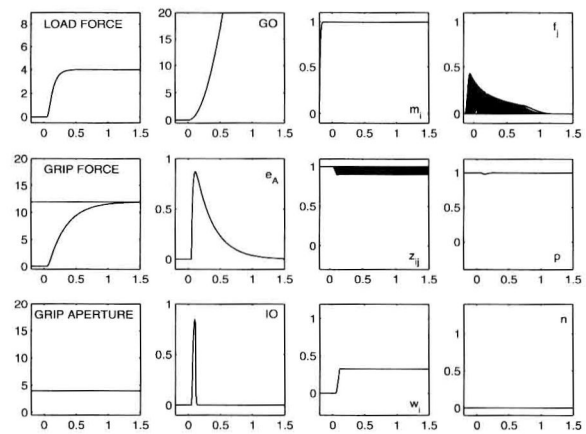

(A)

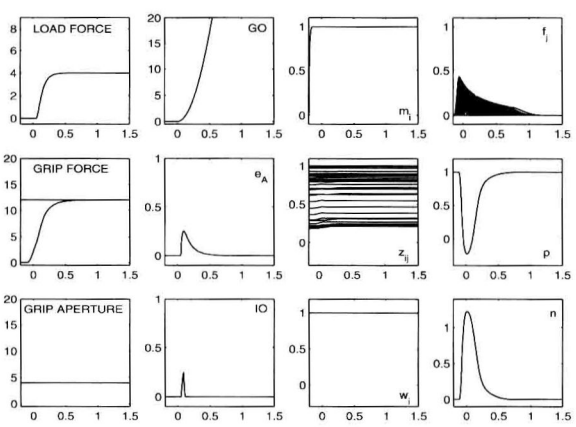

(B)

Fig. 2. (A) Single trial evolution of model variables during early phase of learning adequate grip forces for a 400g silk-covered object. Horizontal axes give time in s; the horizontal line in the grip force plot shows the minimal grip force necessary to prevent slip. Key: e_A, delayed slip error; IO, inferior olive discharge $h(e_A)$; m_i, mossy fiber activity; z_{ij}, adaptive parallel fibers-Purkinje cell synapses; w_i, adaptive mossy fiber-nuclear cell synapse; f_j, activities in parallel fibers; p, Purkinje cell activity; n, nuclear cell activity. In the f_j and z_{ij} plots, there are many separate traces that partially superpose. Separation of the z_{ij} values begins to occur just after the IO discharge. (B) Evolution of model variables during one trial following asymptotic learning of grip force generation for same object as in A.

5. Results

To show activation dynamics of key internal variables, simulations of initial learning (Fig. 2A) and asymptotic phases (Fig. 2B) are shown. The behavioral effect of learning can be seen by comparing the early learning plots in Fig. 2A with the asymptotic performance plots in Fig. 2B. Note that although the GO signal takes off at $t = 0$, load force and grip force take off (during early learning) with a lag corresponding to the delay in the error signals ($t = 0.050$ s). During early learning, grip force is increased in *reaction* to load force, whereas after learning grip force onset *precedes* load force onset. Grip aperture, which equals object width, remains the same in all stages of learning. The slip error (e_A), which is large during learning, becomes small after learning. The panel labeled *IO* shows how the model processes the slip error to use only its leading edge to gate cerebellar learning. The functional generation of the adaptive response is seen by an evolution from no pause in activity to a deep pause in the Purkinje cell activity (p), which controls the DCN cell activation (n). The DCN cell is released from inhibition at the moment of the Purkinje cell pause and in proportion to the depth of the pause. The learning that enables the adaptive response can be appreciated by looking at the weights of the PF-Purkinje cell adaptive synapses (z) and the weights of the MF-nuclear cell adaptive synapses (w). In each case, $w_i = 1.0$ after learning, whereas the below 1.0 deviations of those z_{ij} associated with appropriately timed PF signals scaled directly with the magnitude of the required grip force, and with the depth of the Purkinje cell pause. That the learned w_i values were constant while the learned z_{ij} values varied with object weight and texture (not shown) indicates that the z_{ij} changes were causative for both adaptive timing and scaling of the amplitude of the cerebellar response.

To show that the model is able to simultaneously store and recall grip force adjustments for different weights and textures, simulations were run with various weights and textures. Each combination of weight and texture was represented by a distinct context cue, C_i, and a distinct GF_S (Eq. (14)) was used for each texture-weight combination. The circuit was able to generate anticipatory grip forces that depended upon the presented cue (Fig. 3). After learning converged, the two sets of weights, z_{ij} and w_i, maintain values that preempt the slip onset for each of the presented cues. When the 400 g objects are presented (Fig. 3A), the anticipatory grip forces are adequate for each of the three textures. As in Fig. 2B, the grip force for each texture begins to grow before the onset of load forces. The DCN cell activation and resultant anticipatory grip force are larger the more slippery the surface, but with equal rise times. Therefore, both the rate of rise of grip force and the final grip force value are larger the more slippery the surface. Fig. 3B shows model performance with different weights but

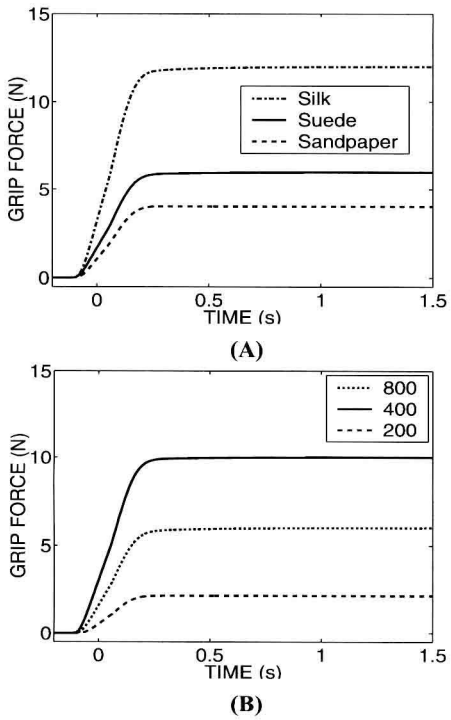

Fig. 3. (A) Simulations of grip force generation for a 400 g object, covered with silk, suede or sandpaper. (B) Simulations of grip force generation for suede-covered objects of three weights (200, 400, and 800 g).

the same texture. Similarly selective, preemptive, error correction can be observed. As in Fig. 2B, the grip force onsets occur in anticipation of load force onset for the three weights. An appropriate grip force is produced, with larger rates of rise and final values for heavier objects, but the grip force rise times for the three weights are equal.

6. Discussion and conclusions

An adaptive circuit was devised to solve the problem of anticipatory application of grip forces when lifting objects of different textures and weights. The cerebellar component of this circuit uses slip signals to adapt the motor commands responsible for exerting just enough force to stabilize the lifted object in the frame of the hand. The adaptive grip force model:

1. Works as a side loop in the aperture control part of a reach–grasp circuit. This circuit makes grip force adjustments in response to slip signals resulting from the application of load forces on the object.
2. Works in anticipation of the activation of the voluntary lifting movement to preempt slippage that would otherwise be produced by that movement. The cerebellar component was able to generate a predictive adjustment to grip force, after the presentation of a context cue corresponding to a visual estimate of object weight and texture. The learned adjustment to grip force was applied in anticipation to load force onset.
3. Resets its compensation when the aperture is voluntarily reset to a larger size, to allow relaxation of the grip aperture.

The cerebellar model of Medina and Mauk (1999) attributed most of the asymptotic memory load in cerebellar learning to the plastic synapse between MFs and DCN cells. Recent data (Hesslow, Svensson, & Ivarsson, 1999) and our results instead suggest that the PF-Purkinje cell synapse can control both timing and amplitude of predictive responses. Our results also accord with the major properties of human grip force adjustment, namely: grip force onset precedes load force onset, grip force and its rate of increase during lifting are functions of object texture and weight, and time to maximum grip force is constant across different weights and textures.

Acknowledgements

A. Ulloa was supported by CONACYT of México (No. 65907); D. Bullock was supported in part by DARPA/ONR N00014-95-1-0409 and NIMH R01 DC02852.

References

Berthier, N., & Moore, J. (1986). Cerebellar Purkinje cell activity related to the classically conditioned nictitating membrane response. *Experimental Brain Research, 63*, 341–350.

Brochier, T., Boudreau, M. J., Pare, M., & Smith, A. M. (1999). The effects of muscimol inactivation of small regions of motor and somatosensory cortex on independent finger movements and force control in the precision grip. *Experimental Brain Research, 128*, 31–40.

Bullock, D., Cisek, P., & Grossberg, S. (1998). Cortical networks for control of voluntary arm movements under variable force conditions. *Cerebral Cortex, 8*, 1–15.

Bullock, D., & Contreras-Vidal, J. (1993). How spinal neural networks reduce discrepancies between motor intention and motor realization. In K. Newell, & D. Corcos (Eds.), *Variability and motor control* (pp. 183–221). Champaign, Il: Human Kinetic Press.

Bullock, D., Fiala, J., & Grossberg, S. (1994). A neural model of timed response learning in the cerebellum. *Neural Networks, 7*, 1101–1114.

Dugas, C., & Smith, A. (1992). Responses of cerebellar Purkinje cells to slip of a handheld object. *Journal of Neurophysiology, 67*, 483–495.

Fagergren, A., Ekeberg, O., & Forssberg, H. (2000). Precision grip force dynamics: a system identification approach. *IEEE Transactions on Biomedical Engineering, 47*, 1366–1375.

Gellman, R., Gibson, A. R., & Houk, J. C. (1985). Inferior olivary neurons in the awake cat: detection of contact and passive body displacement. *Journal of Neurophysiology, 54*, 40–60.

Gordon, A., Westling, G., Cole, K., & Johansson, R. (1993). Memory representations underlying motor commands used during manipulation of common and novel objects. *Journal of Neurophysiology, 69*, 1789–1796.

Hansel, C., Linden, D. J., & D'Angelo, E. (2001). Beyond parallel fiber LTD: the diversity of synaptic and non-synaptic plasticity in the cerebellum. *Nature Neuroscience*, *4*, 467–475.

Hesslow, G., Svensson, P., & Ivarsson, M. (1999). Learned movements elicited by direct stimulation of cerebellar mossy fiber afferents. *Neuron*, *24*, 179–185.

Ito, M. (1984). *The cerebellum and neural control*. New York: Raven Press.

Johansson, R. (1996). Sensory control of dexterous manipulation in humans. In A. Wing, P. Haggard, & J. Flanagan (Eds.), *Hand and brain: The neurophysiology and psychology of hand movements* (pp. 381–414). London: Academic Press.

Johansson, R., & Westling, G. (1984). Roles of glabrous skin receptors and sensorimotor memory in automatic control of precision grip when lifting rougher or more slippery objects. *Experimental Brain Research*, *56*, 550–564.

Johansson, R., & Westling, G. (1987). Signals in tactile afferents from the fingers eliciting adaptive motor responses during precision grip. *Experimental Brain Research*, *66*, 141–154.

Johansson, R., & Westling, G. (1988). Coordinated isometric muscle commands adequately and erroneously programmed for the weight during lifting task with precision grip. *Experimental Brain Research*, *71*, 59–71.

Lemon, R., Johansson, R., & Westling, G. (1995). Cortico-spinal control during reach, grasp, and precision lift in man. *Journal of Neuroscience*, *15*, 6145–6156.

Maier, M. A., Bennett, K. M., Hepp-Reymond, M. C., & Lemon, R. N. (1993). Contribution of the monkey corticomoto-neuronal system to the control of force in precision grip. *Journal of Neurophysiology*, *69*, 772–785.

Medina, J., & Mauk, M. (1999). Simulations of cerebellar motor learning: Computational analysis of plasticity at the mossy fiber to deep nucleus synapse. *Journal of Neuroscience*, *19*, 7140–7151.

Passingham, R. (1993). *The frontal lobes and voluntary action*. Oxford: Oxford University Press.

Rhodes, B., & Bullock, D. (2002). A scalable model of cerebellar adaptive timing and sequencing: The recurrent slide and latch (RSL) model. *Applied Intelligence*, *17*, 35–48.

Serrien, D. J., & Wiesendanger, M. (1999). Role of the cerebellum in tuning anticipatory and reactive grip force responses. *Journal of Cognitive Neuroscience*, *11*, 672–681.

Smith, A., & Bourbonnais, D. (1981). Neuronal activity in cerebellar cortex related to control of prehensile force. *Journal of Neurophysiology*, *45*, 286–303.

Thach, W., Goodkin, H., & Keating, J. (1992). The cerebellum and the adaptive coordination of movement. *Annual Review of Neuroscience*, *15*, 403–442.

Ulloa, A., & Bullock, D. (2003). A neural network simulating human reach–grasp coordination by continuous updating of vector positioning commands. *Neural Networks*.

Vilis, T., & Hore, J. (1980). Central neural mechanisms contributing to cerebellar tremor produced by perturbations. *Journal of Neurophysiology*, *43*, 279–291.

Westling, G., & Johansson, R. (1984). Factors influencing the force control during precision grip. *Experimental Brain Research*, *53*, 277–284.

Wing, A. (1996). Anticipatory control of grip force in rapid arm movement. In A. Wing, P. Haggard, & J. Flanagan (Eds.), *Hand and brain: The neurophysiology and psychology of hand movements* (pp. 301–324). London: Academic Press.

PERGAMON

AVAILABLE AT
www.ComputerScienceWeb.com
POWERED BY SCIENCE DIRECT

Neural Networks 16 (2003) 529–535

Neural Networks

www.elsevier.com/locate/neunet

2003 Special issue

Radial basis function neural networks for nonlinear Fisher discrimination and Neyman–Pearson classification

David Casasent[a,*], Xue-wen Chen[b]

[a]*Department of Electrical and Computer Engineering, Carnegie Mellon University, Pittsburgh, PA 15213, USA*
[b]*Department of Electrical and Computer Engineering, California State University, Northridge, CA 91330, USA*

Abstract

We propose a novel technique for the design of radial basis function (RBF) neural networks (NNs). To select various RBF parameters, the class membership information of training samples is utilized to produce new cluster classes. This allows emphasis of classification performance for certain class data rather than best overall classification. This allows us to control performance as desired and to approximate Neyman–Pearson classification. We also show that by properly choosing the desired output neuron levels, then the RBF hidden to output layer performs Fisher discrimination analysis, and that the full system performs a nonlinear Fisher analysis. Data on an agricultural product inspection problem and on synthetic data confirm the effectiveness of these methods.

Keywords: Clustering; Linear discriminant analysis; Neural networks; Neyman–Pearson classification; Radial basis function networks

1. Introduction

Radial basis function (RBF) neural networks (NNs) are attractive due to their fast training and simplicity. They have been used in function approximation (Poggio & Girosi, 1990) [1], pattern recognition (Krzyzak, Linder, & Lugosi, 1996), and signal processing (Chen, Mulgrew, & Grant, 1993). An important consideration in designing RBF networks is the hidden layer (Billings & Zheng, 1995; Bruzzone & Prieto, 1998; Chen, Cowan, & Grant, 1991; Moody & Darken, 1989; Musavi, Ahmed, Chan, Faris, & Hummels, 1992; Vogt, 1993). Much work exists (Moody & Darken, 1989; Musavi et al., 1992; Vogt, 1993; Bruzzone & Prieto, 1998) using clustering to select the RBFs to use. The original RBF NNs (Poggio and Girosi, 1990) were concerned with representing nonlinear mapping functions by RBF interpolation; thus clustering methods used were different and many RBF neurons were used. For classification applications, a large number of RBFs are not desirable for on-line computational reasons and for good generalization (similar training and test set scores). Most of the clustering methods (Moody & Darken, 1989; Vogt, 1993) used in RBF NNs did not consider the class of the samples when clustering (this is not attractive for a classification application). For classification applications, other RBF cluster selection methods are needed. For classification applications, others (Bruzzone & Prieto, 1998; Musavi et al., 1992) allow clusters with very few samples (this produces poor mean and variance estimates and poor generalization).

Another issue, which is not considered in most work, is the effect of the choice of the desired outputs on system performance. Different choices result in different performance (Bishop, 1995). For two-class cases, a common choice of the desired outputs is 1 for one class and 0 for the other. With this choice and the mean square error cost function, the output neuron level can be the posterior probability (Richard & Lippmann, 1991) that the input is in class 1 or 2. However, practical networks are often far from ideal estimators due to the fact that the training data is not sufficient to specify the network and that the network is not sufficiently complex to model the posterior distribution accurately. Therefore, the choice [0,1] does not necessarily minimize the probability of error.

There are many applications in which minimizing the probability of error is not the best criterion to design a decision rule because the misclassifications of samples from different class may have different consequences. For example, in agricultural product inspection problems, the goal is to reduce the amount of bad products to some level while not removing more than a certain percentage of the good products. The Neyman–Pearson (N-P) criterion

* Corresponding author. Tel.: +1-412-268-2464; fax: +1-412-268-6345.
E-mail address: casasent@ece.cmu.edu (D. Casasent).

0893-6080/03/$ - see front matter
doi:10.1016/S0893-6080(03)00086-8